COMPUTERS AND BIOMEDICAL RESEARCH **31,** 271–292 (1998)
ARTICLE NO. CO981481

Comparative Study of Local and Karhunen–Loève-Based ST–T Indexes in Recordings from Human Subjects with Induced Myocardial Ischemia

José García,*[,1] Paul Lander,† Leif Sörnmo,‡ Salvador Olmos,*
Galen Wagner,§ and Pablo Laguna*

**Grupo de Tecnologías de las Comunicaciones, Departamento de Ingeniería Electrónica y Comunicaciones, Centro Politécnico Superior, Universidad de Zaragoza, 50015 Zaragoza, Spain; ‡Signal Processing Group, Department of Applied Electronics, University of Lund, Lund, Sweden; †VA Medical Center, University of Oklahoma, Oklahoma City, Oklahoma 73190; and §Department of Medicine, Division of Cardiology, Duke University Medical Center, Durham, North Carolina 27708*

Received November 18, 1997

In this work we studied ST–T complex changes in the ECG as result of induced ischemia. The principal aim was to determine whether global changes in the ST–T complex were more sensitive markers of ischemic alterations than those based on measurements of changes at specific locations on ST segment or T wave. High-resolution ECGs from patients undergoing percutaneous transluminal coronary angioplasty in one of the major coronary arteries were analyzed to give a description of the period from the end of active depolarization (QRS complex) to the end of active repolarization (T wave). During artery occlusion traditional local measurements of the ST–T complex were compared to global measurements based on the Karhunen–Loève transform. An ischemic change sensor parameter was estimated for each of the studied indexes showing that global measurements detected changes better in the repolarization period in a larger number of leads and with higher sensitivity (more than 85%) than was done using local measurements (sensitivity of 64% with ST level, 33% with T-wave maximum position, and 37% with T-wave maximum amplitude). Using these global indexes it was found that most cases of ST-segment changes were accompanied by T-wave changes (72% of patients). With the use of traditional indexes 23% of patients showed no changes in the repolarization period, whereas with global indexes this percentage decreased to 8%. Thus a global representation of the entire ST–T complex appears to be more suitable than local measurements when studying the initial stages of myocardial ischemia.

INTRODUCTION

Myocardial ischemia is caused by a lack of oxygen to the contractile cells. The transient occlusion of a coronary artery can result in reversible ischemia, and a prolonged obstruction may lead to myocardial infarction with its severe sequelae

[1] To whom correspondence should be addressed at Departamento de Ingeniería Electrónica y Comunicaciones, Centro Politécnico Superior, Universidad de Zaragoza, C/María de Luna, 3, 50015 Zaragoza, Spain. Fax: +34-976 762111. E-mail: jogarmo@posta.unizar.es.

0010-4809/98 $25.00

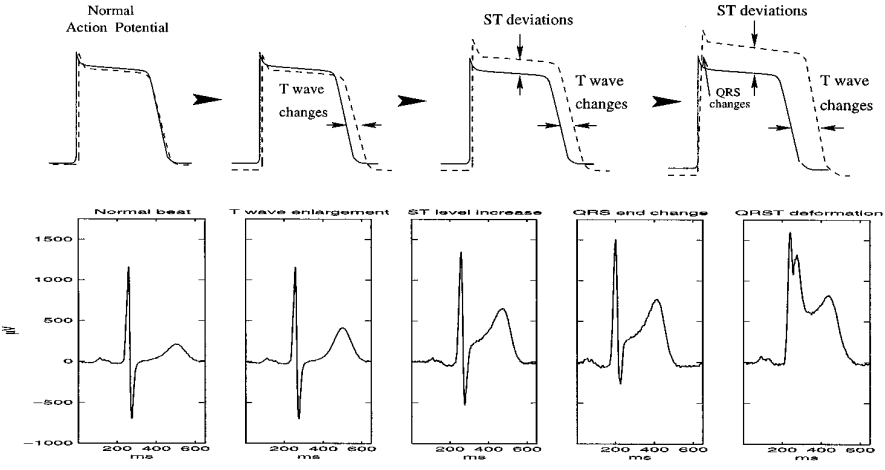

FIG. 1. Normal (solid lines) and abnormal (dashed lines) hypothesized ventricular action potentials during transmural ischemia induced by complete coronary occlusion are represented at the top. A possible evolution of the ECG waveform along PTCA is simulated at the bottom.

of heart failure and arrhythmias and maybe even patient death. The ST–T complex of the ECG reflects the time period from the end of active ventricular depolarization to the end of repolarization in the electrical cardiac cycle. Further, the ST segment is influenced by resting potential, particularly in the setting of acute ischemia. Ischemia is usually quantified in the standard ECG by changes in values of measured amplitudes, times, and durations on the ST–T complex. Different stages of the severity of ischemic progression have been described (*1*): the first stage is characterized by T-wave amplitude increase without simultaneous ST segment change. Second, as the ischemia extends transmurally through the myocardium, the intracellular action potential shortens and the injured cells become hyperpolarized, producing an ''injury current'' that is shown as horizontal ST segment deviation. At the last stage the ischemia is so extensive that the terminal portion of the active depolarization waveform (QRS complex) is altered. Previously alterations in the QRS complex had traditionally been associated with myocardial necrosis. A model evolution of ventricular action potentials during an ischemic process can be seen at the top of Fig. 1 and, at the bottom, a simulated ECG ischemic progression is shown.

Percutaneous transluminal coronary angioplasty (PTCA) provides an excellent model to investigate the electrophysiological changes of transmural ischemia. The sudden complete coronary occlusion produced by balloon angioplasty allows the study of the initial minutes of the ischemic process that would eventually lead to acute myocardial infarct (2). Several studies have shown different ECG changes evoked by PTCA when the occlusion was prolonged (*3–5*).

Most of the commonly used indexes in cardiology are based on single local

measurements on the ECG: ST segment deviations (*6*, *7*), QT variability (*8–10*), repolarization alternans (*11*, *12*), etc. However, there is not a test reported in the literature which can robustly detect the presence, extent, and severity of ischemia in monitoring applications.

The Karhunen–Loève transform (KLT) has previously been studied in ECG signal processing (*13–15*). The KLT was used in the study of spatial and temporal compression of body surface potential maps (*16*, *17*) and recently in ECG data compression (*18*), improving the results of other orthogonal transforms. In a precedent work (*19*), the KLT was successfully applied to analyze the ST segment of the ECG, with the specific aim of obtaining noise-tolerant methods for ischemia detection. The KLT was recently applied to the entire ST–T complex in ischemic changes monitoring (*20*).

Traditionally the ECG is studied by means of measurements at specific points of it, e.g., ST level. We call them local indexes. On the other hand, we call global indexes the measurements that take into account the information contained in a segment of the ECG signal, e.g., the KL-based indexes. In this work we want to study the global changes of the entire ST–T complex during the inflation period of PTCA and compare these with the traditional measurements of ST segment and T wave (position and amplitude) from the standard ECG. We study a new way to evaluate myocardial ischemia on the ECG based on the KLT applied to the entire ST–T complex to include as much information about the ventricular repolarization period as possible (including not only ST segment deviations but T wave changes as well). First we will describe how the KLT is applied to the different ECG segments and how the KL-based indexes are obtained. Then we will define a parameter that will permit the comparison of the indexes' sensitivity for induced ischemia detection. We will also study the incidence of ischemia on the different ECG intervals.

MATERIALS AND METHODS

Study Population and ECG Acquisition

The study group consisted of 108 patients receiving elective prolonged PTCA in one of the major coronary arteries at the Charleston Area Medical Center in West Virginia. Twenty-five patients were excluded because they had ventricular tachycardia, underwent an emergency procedure, or demonstrated signal loss during the acquisition. A total of 92 dilations in 83 patients (55 males, 28 females) were included in this study. The inflation times ranged from 1 min 30 s to 7 min 17 s (mean 4 min 23 s). Notice the long mean period of occlusion compared to a normal procedure. The locations of the 92 dilations were left anterior descending artery in 30 patients, right coronary artery in 39 patients, and left circumflex artery in 23 patients. Nine leads (V1–V6, I, II, and III) were recorded using equipment by Siemens–Elema AB (Solna, Sweden) and digitized at a sampling rate of 1000 Hz and amplitude resolution of 0.6 μV. One or two control ECGs (in the room and/or catheterization laboratory) prior to the procedure and several postinflation ECGs were recorded for each patient.

Karhunen–Loève Transform

The KLT is an orthogonal linear transform which is optimal in the sense that it concentrates the signal information in the minimum number of parameters (in the mean square error (MSE) sense) (*21*). The KLT is a signal-dependent transform and must be derived from the statistics of the signals to be analyzed. Thus, the KLT requires that a representative "training set" of signals is collected to obtain the KLT basis functions (eigenfunctions). The KLT can be understood as a rotational transformation of a pattern vector (the signal vector to be represented) into a feature vector, composed by the KL coefficients. The first few components of the coefficients vector represent almost all the signal energy. The KLT basis functions are derived from the covariance matrix **C** of the training set estimated as

$$\mathbf{C} = \mathcal{E}\{(\mathbf{x} - \mathbf{m})(\mathbf{x} - \mathbf{m})^{\mathrm{T}}\}, \qquad [1]$$

where $\mathbf{x} = [x(0), \ldots, x(N-1)]$ represents each signal vector in the training set (in this work it will be each ST segment, T wave, or ST–T complex), **m** is the mean pattern vector over the entire training set, and $\mathbf{x}^{\mathrm{T}}$ is the transpose of **x**. The orthogonal eigenvectors of **C** are the basis functions of the KLT, and the eigenvalues represent the average dispersion of the projection of a pattern vector onto the corresponding basis function. When the basis functions are obtained, each signal vector **x** is represented in the KL space by the coefficients vector $\alpha' = [\alpha'_0, \alpha'_1, \ldots, \alpha'_{N-1}]^{\mathrm{T}}$ (α' indicates that it is a nonnormalized vector, calculated as

$$\alpha'_i = \sum_{k=0}^{N-1} \phi_i(k)x(k), \qquad [2]$$

with ϕ_i representing the ith order KL basis function and **x** the signal vector (in our case the analyzed complex or wave) with length N.

The dynamic evolution of the signal can be characterized by the study of the coefficient time series, $\alpha_i(n)$, where i is the series order and n is the occurrence time order. The time series $\alpha_i(n)$ can also be normalized with respect to a constant value given by the square root of a template signal vector energy and estimated as

$$\alpha_i(n) = \frac{\sum_{k=0}^{N-1} \phi_i(k)x_n(k)}{(E_{n_0})^{1/2}}, \qquad [3]$$

where E_{n_0} is the energy of the template vector ($\mathbf{x}_{n_0}$). The use of the template normalization permits the quantitative interpretation of different KL series, with respect to the template beat coefficients.

An adaptive transversal algorithm can be used to remove noise which is uncorrelated to the signal (*22*). When the LMS algorithm is used in the estimation of the $\alpha_i(n)$ series the time constant for the convergence of the MSE is

$$\tau_{\mathrm{mse}} = \frac{N}{4\mu} \quad \text{(samples)}, \qquad [4]$$

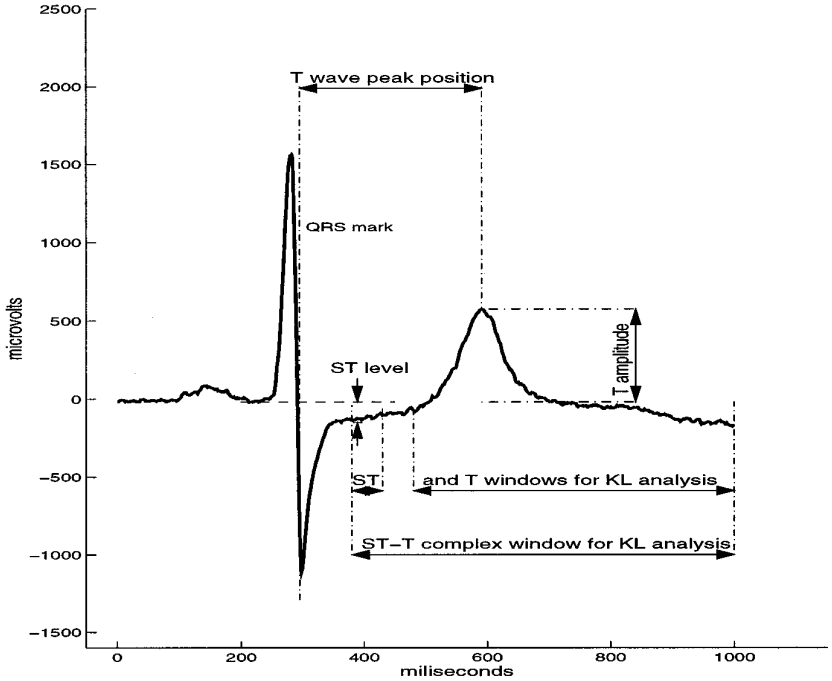

FIG. 2. Local and global measurements.

where μ is the step-size parameter of the LMS algorithm and N is the length (number of samples) of the signal. The steady-state signal-to-noise ratio improvement (ΔSNR) in the $\alpha_i(n)$ series estimation obtained using the adaptive filter (*22*) is approximately

$$\Delta\text{SNR}_{\text{LMS}} \simeq \frac{1}{\mu}. \qquad [5]$$

The classical trade-off between convergence time (tracking capability) and signal-to-noise ratio improvement (related to the misadjustment) appears with the selection of the LMS step-size parameter.

For a given signal vector $\mathbf{x}_n$ it is possible to calculate the percentage of energy represented by the ith coefficient, $E_n^{\text{P}}(i) = 100\ \mathcal{N}\alpha_i^2(n)$, and the percentage of cumulative represented energy, $E_n^{\text{C}}(i) = 100\ \mathcal{N}\ \sum_{p=0}^{i-1}\alpha_p^2(n)$, where $\mathcal{N} = E_{n_0}/E_n$ is the normalization constant that arises from the template normalization energy. Obviously with the N KL basis functions it is possible to represent the signal vector completely and $\sum_{i=0}^{N-1} E_n^{\text{P}}(i) = E_n^{\text{C}}(N) = 100\%$.

In this work we have studied three ECG intervals (ST segment, T wave, and the entire ST–T complex) for the detection of ischemic changes. The different windows used in the KL basis functions derivation and $\alpha_i(n)$ series estimation are represented in Fig. 2. For the ST segment window we used the first 50 ms

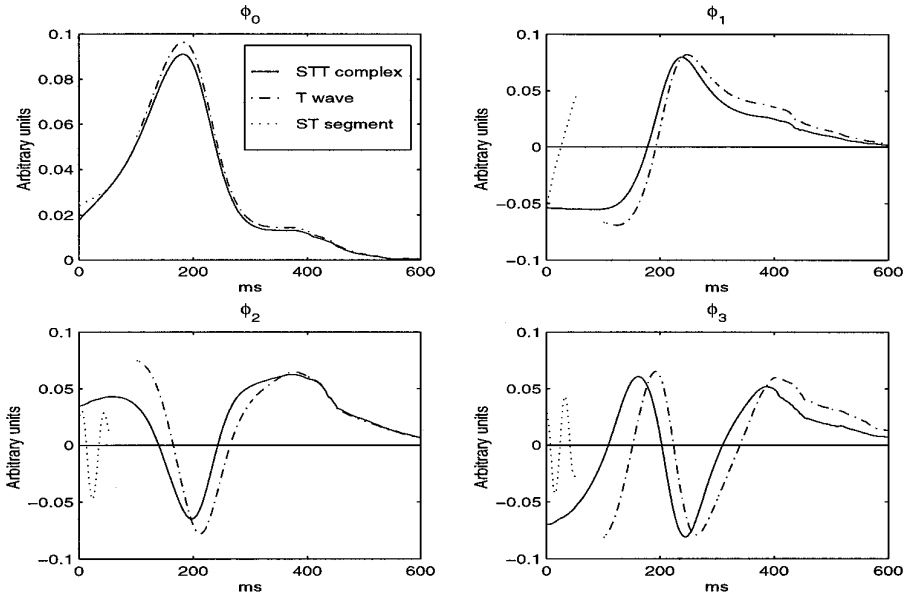

FIG. 3. First four KL basis functions of ST–T complex ($\phi_0^{\mathrm{STT}}, \ldots, \phi_3^{\mathrm{STT}}$) in solid lines, T wave ($\phi_0^{\mathrm{T}}, \ldots, \phi_3^{\mathrm{T}}$) in dash-dotted lines, and ST segment ($\phi_0^{\mathrm{ST}} \ldots, \phi_3^{\mathrm{ST}}$) in dotted lines.

of the ST–T complex window, whose beginning is referred to a fixed distance (85 ms) from the QRS fiducial point detected by Aristotle (*23*). The beginning of the T-wave window was selected 100 ms from the ST–T complex window beginning, and the end of the T-wave (and ST–T complex) window was selected depending on the heart rate (HR). The training set used in this study was obtained from the QT database (*24*) that is composed of signals including different T-wave shapes, ST deviation patterns, etc. Signal preprocessing (including selection of beats labeled as normal according to Aristotle (*23*), cubic splines baseline wander rejection (*25*), and correction for the effects of the HR using Bazett's formula (*26*)) was applied in the derivation of the basis functions. Each set of eigenfunctions (for ST segment, T wave, and ST–T complex) was derived using more than 200,000 preprocessed and selected waveforms (coming from a two-leads ECG recorder). The first four KL basis functions derived for the T wave (ϕ_i^{T}), ST segment (ϕ_i^{ST}), and ST–T complex (ϕ_i^{STT}) can be seen in Fig. 3.

In Fig. 4 the reconstruction of a ST–T complex (the ST–T complex template selected for the energy normalization) using different numbers of α_i^{STT} coefficients is shown. These values and the percentage of energy represented by each coefficient, $E_n^{\mathrm{P}}(i)$, and the percentage of cumulative represented energy, $E_n^{\mathrm{C}}(i)$, appear in the table of Fig. 4. The two first coefficients have the largest representation strength, and with four $\alpha_i(n)$ coefficients more than 90% of the signal energy is represented.

order	$\alpha_i^{STT}(n_0)$	$E_{n_0}^P(i)$	$E_{n_0}^C(i)$
i=0	0.75	55.9 %	55.9 %
i=1	-0.46	21.3 %	77.2 %
i=2	-0.22	6.7 %	83.9 %
i=3	0.26	6.8 %	90.7 %

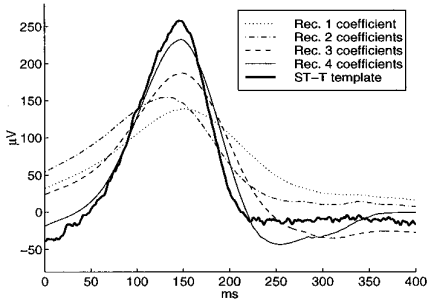

FIG. 4. Left: template beat coefficients ($\alpha^{\mathrm{STT}}(n_0)$), energy, and cumulative energy are represented. Right: graphic reconstructions of the ST–T complex template ($\mathbf{x}_{n_0}$) with one to four α^{STT} coefficients.

Each $\alpha_i(n)$ series of the different windows was estimated by normalizing with respect to the square root of the complex energy of the template beat selected for the entire study (see Fig. 4). From the definition of the $\alpha_i(n)$ series given in Eq. [3] it is evident that a given beat with smaller $\alpha_i(n)$ coefficients (in absolute value) than those of the template beat will have less energy. Furthermore the deviations of its coefficients' values from those of the template beat will give information about the differences between the analyzed and the template beats related to the basis functions shape; e.g., a smaller (in absolute value) $\alpha_i^{\mathrm{STT}}(n)$ coefficient than that corresponding to the template beat, $\alpha_i^{\mathrm{STT}}(n_0)$, means that the ϕ_i^{STT} basis function (Fig. 3) has a smaller contribution and representation strength in the analyzed beat than in the template beat. For T wave or ST segment the description is similar.

With the first two to four $\alpha_i(n)$ coefficients series it is possible to represent 70–90% of the complex energy (*20*). In the next computer simulations it will be seen that it is also possible to track ST segment, T-wave, or ST–T changes following the evolution of the estimated series for each interval.

Computer Simulations and Series Interpretation

The capability of the KL series to represent repolarization changes was studied by means of different computer simulations of: (a) ST level depression and (b) T-wave morphology changes without significant ST level change. These simulations show that the first two $\alpha_i(n)$ series are sufficient to track morphology changes in the repolarization period. The first simulation, corresponding to a ST-level depression of approximately 150 μV in combination with a small decrease of T-wave amplitude (50 μV), can be seen in Fig. 5. The top shows the evolution of the ST–T complex shape along the ischemia simulation and the bottom the first four $\alpha_i(n)$ time series of ST–T complex. It is evident that the largest changes occur in the first two series, which have also the maximum representation strength (the percentage of represented energy, $E_n^{\mathrm{p}}(i)$, is high for the first two series ($i = 0, 1$), whereas $\alpha_2^{\mathrm{STT}}(n)$ and $\alpha_3^{\mathrm{STT}}(n)$ remain with relatively

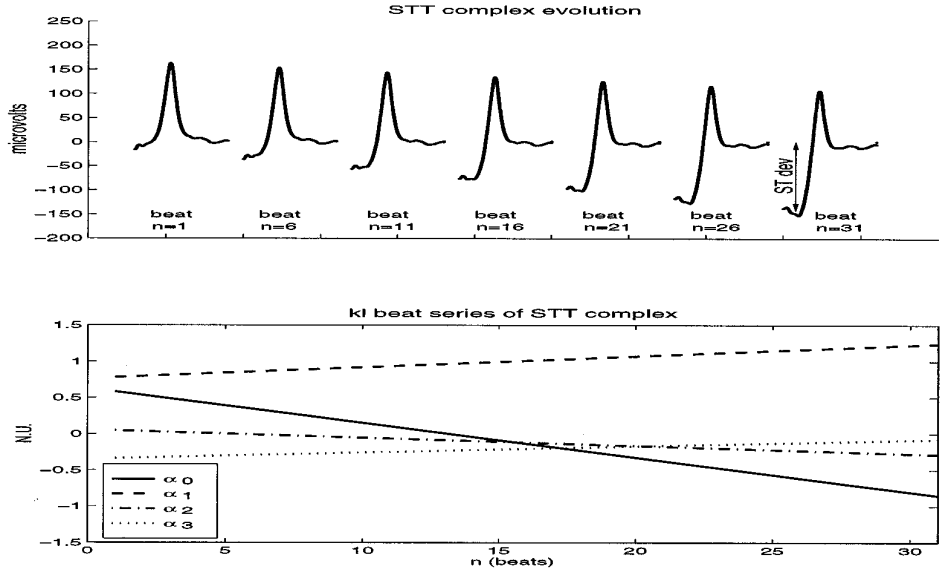

FIG. 5. Simulation of ST-level changes.

low values during the ischemia simulation). The $\alpha_0^{\mathrm{STT}}(n)$ series has a negative slope, corresponding to a decrease in the ST level. This can be corroborated by inspection of the first basis function, ϕ_0^{STT} (see Fig. 3). The second series presents smaller changes and its positive slope is due to the shape of ϕ_1^{STT} basis function (see Fig. 3) that takes negative values in the region of ST segment. The remaining coefficient series show even smaller changes. In Fig. 6 the computer simulation of T-wave changes is shown. In this example the T wave is approaching the QRS complex in combination with an increase of its amplitude but without significant changes in ST level (less than 50 μV). The evolution of the ST–T complex is shown in the top of Fig. 6, starting with a T-wave maximum amplitude and position relative to the QRS fiducial point, $T_{\mathrm{a}} = 160$ μV and $T_{\mathrm{p}} = 315$ ms, respectively, and with values at the end of the occlusion of $T_{\mathrm{a}} = 300$ μV and $T_{\mathrm{p}} = 210$ ms. The $\alpha_i(n)$ time series of the ST–T complex evolution for the first four coefficients are shown in the bottom of Fig. 6, reflecting the induced changes. The first two KL series ($\alpha_0^{\mathrm{STT}}(n)$ and $\alpha_1^{\mathrm{STT}}(n)$) show again the largest changes. The $\alpha_0^{\mathrm{STT}}(n)$ time series reflects an increase that corresponds (by inspection of the ϕ_0^{STT} basis function in Fig. 3) to an increase of the ST–T complex amplitude and a displacement toward the QRS. The decrease in $\alpha_1^{\mathrm{STT}}(n)$ can be related to the same behavior of ST–T complex evolution. If changes in ST level (elevation/depression) as well as T-wave variations were present, $\alpha_i(n)$ trends of ST–T complex could show even larger variations with respect to its reference values. From these two simulations it seems clear that the first two $\alpha_i(n)$ series permit tracking of ST–T complex changes.

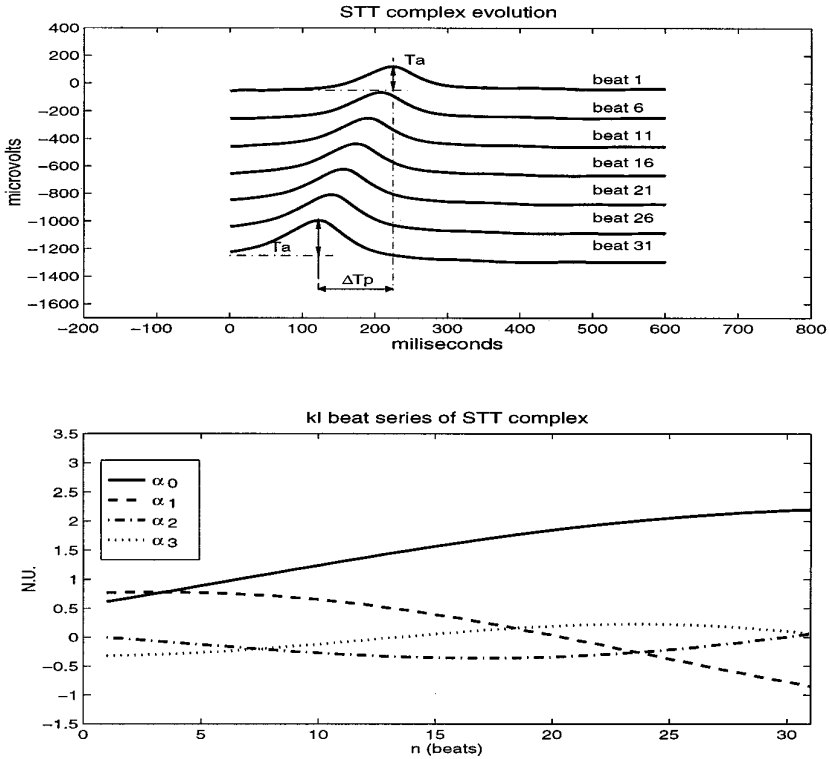

FIG. 6. Simulation of T-wave changes.

Local Measurements of the Repolarization Period

We considered several measurements at specific points of the ECG that are traditionally used in clinical diagnosis. The parameter usually estimated in the ventricular repolarization period is the ST segment level. T wave was characterized by T-wave maximum amplitude and position with respect to the QRS (see Fig. 2).

Signal preprocessing (including selection of beats labeled as normal according to Aristotle (*23*), cubic splines baseline wander rejection (*25*), and signal averaging (*27*)) was applied before measuring ST level and T-wave parameters. We averaged the ECG in subensembles of eight beats to get convergence time similar to that obtained when the KL method is adaptively applied with a signal-to-noise ratio improvement of $\Delta SNR = 15$ dB.

On the continuously averaged ECG we measured the traditional indexes as described below. The ST level was estimated to a fixed distance from the QRS fiducial point detected by Aristotle (*23*) that roughly yields the commonly used ST60 measurement. The maximum amplitude and position of T wave were

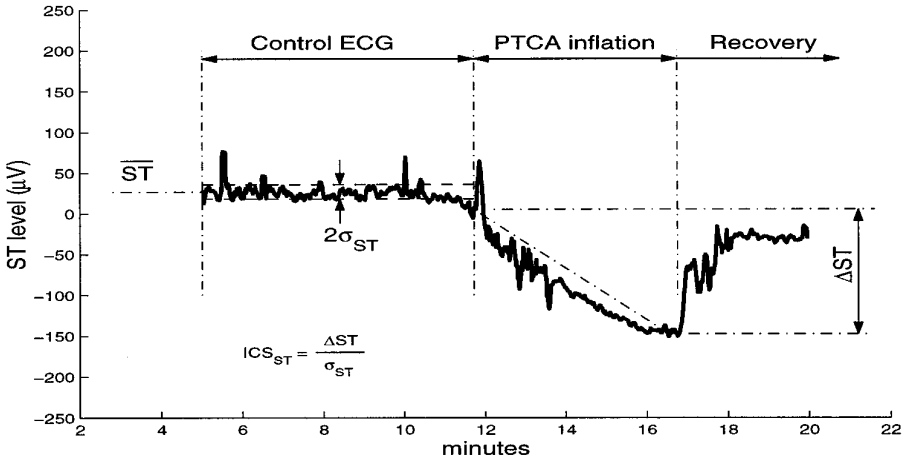

FIG. 7. Example of series evolution and ICS parameter derivation corresponding to ST(*n*) series.

measured using the waveform limits detector described in (*28*) and recently validated with expert cardiologists (*29*). The location of T-wave maximum (or minimum if it is inverted) is performed at the zero crossing of the low-pass differentiated signal. The maximum amplitude was estimated using as reference the isoelectric level between *P*-wave end and QRS onset (averaging 10 ms of this segment). T-wave maximum position (or RTm distance) was measured using the QRS fiducial point as reference point (see Fig. 2).

The Ischemic Changes Sensor Parameter

An ischemic changes sensor (ICS) parameter was defined and estimated for every studied index to compare its capability of detecting ischemic changes. This ICS parameter should provide information on the magnitude of changes that the corresponding index reflects. It was defined as

$$\mathrm{ICS}_{\mathrm{index}} = \frac{\Delta\mathrm{index}}{\sigma_{\mathrm{index}}}, \qquad [6]$$

where Δindex is the magnitude of change in each index during PTCA occlusion, σ_{index} is the standard deviation of the index measured in the control ECG, and index can be any of ST, T_p, T_a, α_0^T, α_1^T, α_0^{ST}, α_1^{ST}, α_0^{STT}, or α_1^{STT}. In Fig. 7 an example which describes how this ICS parameter was developed is shown (the example corresponds to a ST(*n*) series). First, we used a control ECG recorded in the room or in the catheterization laboratory (previous to the inflation) to measure the standard deviation of changes. This value would reflect normal changes of ECG indexes, and thus changes during PTCA of the same order as σ_{index} should not be considered significant. The control interval usually was 5

min long (the same order as the mean inflation time). During the occlusion period the magnitude of change in each index, Δindex, was estimated applying a linear fitting model (see Fig. 7). When the absolute magnitude of changes is smaller than the standard deviation ($|\Delta\text{index}| < \sigma_{\text{index}}$) the factor is smaller than unity, and the larger the changes during the inflation the larger is the factor (in absolute value). Also, the ICS parameter sign permits one to distinguish between increase and decrease of the index during the occlusion. For example, a value of $\text{ICS}_{\text{ST}} = -10$ means that the ST segment level has decreased during the occlusion 10 times its σ_{ST} value, i.e., 10 times its normal change during the control recording.

To define a decision rule that shows when repolarization changes had been detected with each of the indexes, we applied a threshold η to the ICS parameter. Significant changes in the index were considered when the threshold was exceeded ($|\text{ICS}_{\text{index}}| > \eta$). For each patient in each lead, we applied this decision rule with several values of η to every index to decide whether a change had occurred.

By means of the $\text{ICS}_{\text{index}}$ we compared the traditional local measurements of ST segment and T wave to the global measurements of ST–T complex based on the KLT to determine which one can be more sensitive to the repolarization changes induced by ischemia. We obtained the trends series for the different indexes evaluated before and during PTCA and the corresponding ICS parameters were estimated.

RESULTS

Sensitivity to Ischemic-Induced Changes

The changes detected in the ventricular repolarization during balloon inflation were studied following the methods described above. The series of ST level ($\text{ST}(n)$), T-wave maximum position ($T_{\text{p}}(n)$), and T-wave maximum amplitude ($T_{\text{a}}(n)$) and the first two KL series for the T wave, ST segment, and ST–T complex ($\alpha_0^{\text{T}}(n)$, $\alpha_1^{\text{T}}(n)$, $\alpha_0^{\text{ST}}(n)$, $\alpha_1^{\text{ST}}(n)$, $\alpha_0^{\text{STT}}(n)$, and $\alpha_1^{\text{STT}}(n)$, respectively) were calculated and the magnitude of changes, Δindex, and ICS parameter were estimated for each index and each lead in every patient.

During prolonged PTCA significant ischemic-induced changes were found. This can be seen in Fig. 8 in which mean and standard deviation (over all the patients) of the different indexes' variations during the occlusion ($\overline{|\Delta\text{index}|}$ and $\sigma_{|\Delta\text{index}|}$, respectively) are shown. These gross statistics were calculated considering variations in absolute value to avoid the cancellation of positive and negative changes among different patients. In Fig. 8a the estimated variations in both ST segment (mean between 29 and 109 μV, depending on the lead, for ST index) and T wave (mean between 34 and 43 ms in maximum position and between 44 and 176 μV in amplitude) are represented. In Figs. 8a and 8b it can be seen that leads V3, V2, V4, and III showed the largest changes in all the series, except in $T_{\text{p}}(n)$ series in which the variations were of the same order for all the leads. The standard deviation of changes (represented as bars attached to the mean values) in the different indexes ($\sigma_{|\Delta\text{index}|}$) are of the same order as the mean change

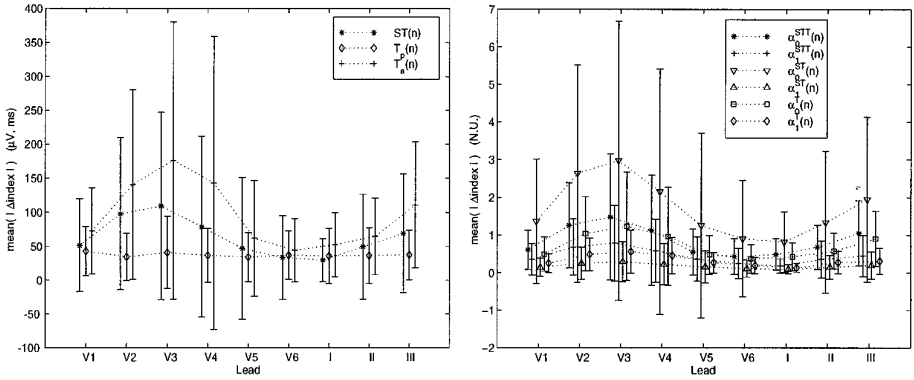

(a) $\overline{|\Delta index|}$ and $\sigma_{|\Delta index|}$ for local indexes.

(b) $\overline{|\Delta index|}$ and $\sigma_{|\Delta index|}$ for KL-derived indexes.

FIG. 8. $\overline{|\Delta\text{index}|}$ and $\sigma_{|\Delta\text{index}|}$ (as attached bars) for the different indexes.

($\overline{|\Delta\text{index}|}$), showing that there were large differences in changes depending on the patient. The α_0 indexes showed larger changes in mean than did the α_1 indexes.

The KL-derived indexes showed larger $|\text{ICS}_{\text{index}}|$ than the local indexes did. The results of $\overline{|\text{ICS}_{\text{index}}|}$ are shown in Figs. 9a and 9b. The $|\text{ICS}_{\text{ST}}|$ parameter also reached high values in mean among patients, but we will see in the averaged sensitivity statistics (patient by patient) the clear prevalence of $\alpha_i(n)$ series over

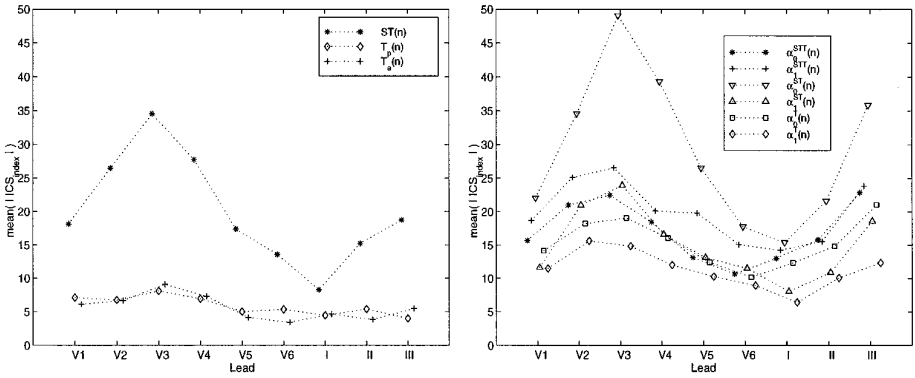

(a) $\overline{|ICS_{index}|}$ for local indexes.

(b) $\overline{|ICS_{index}|}$ for KL-derived indexes.

FIG. 9. $\overline{|\text{ICS}_{\text{index}}|}$ for the different indexes.

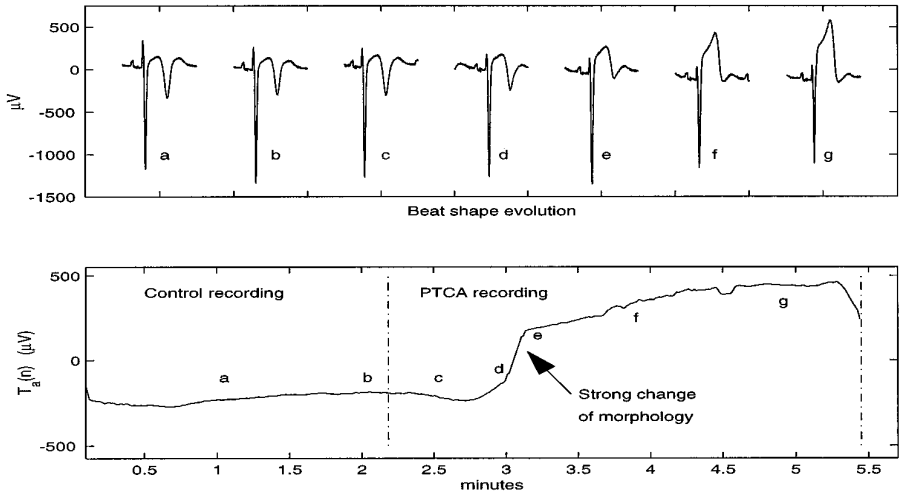

FIG. 10. Strong morphology changes in T wave during PTCA are shown at the top. The bottom reflects the corresponding step change reflected in $T_a(n)$ series (the time interval between dash-dotted lines corresponds to the occlusion period).

the rest of indexes in the ischemia detection. The largest values of $\overline{|\mathrm{ICS}_{\mathrm{index}}|}$ were found again in leads V3, V2, V4, and III.

T-wave changes during PTCA that were accompanied by strong shape variations (including polarity inversions, changes from monophasic to biphasic waves, etc.) were detected by inspection of T-wave maximum amplitude and position series; e.g., when T-wave inversion or a phase change has occurred, a step change in $T_a(n)$ or $T_p(n)$ series, respectively, is often seen. In 32 dilations (35%) strong shape variations of T wave were found during the induced ischemia in at least one lead, showing that the repolarization period was affected with significant morphology changes in T wave. In Fig. 10 it is possible to see an example of T-wave amplitude trends ($T_a(n)$) that reflects a step change as a result of the T-wave inversion during the occlusion.

The decision rule was applied with different η values to the ICS parameter obtained for every index as we have described before ($|\mathrm{ICS}_{\mathrm{index}}| > \eta$). In Fig. 11 we can see the sensitivity to the ischemic-induced changes obtained for the different studied indexes (and combinations of them), i.e. the percentage of patients that reflected changes in the different indexes (selecting $\eta = 4$). As the different order $\alpha_i(n)$ series do not have redundant information (because the KLT is an orthogonal transform) we also considered the sensitivity by using a combination of two indexes: $\alpha^{\mathrm{STT}}_{(0,1)}$, $\alpha^{\mathrm{ST}}_{(0,1)}$, and $\alpha^{\mathrm{T}}_{(0,1)}$. In those cases an ischemic change was considered when either one or both indexes exceeded the η threshold. We also show the results of sensitivity for a combination of quasi-orthogonal leads (detection in I or III or V2 leads), represented as QO lead. The $\alpha^{\mathrm{STT}}_{(0,1)}$ index (logical OR combination of α^{STT}_0 and α^{STT}_1 indexes) showed the largest sensitivity in the ischemic-induced

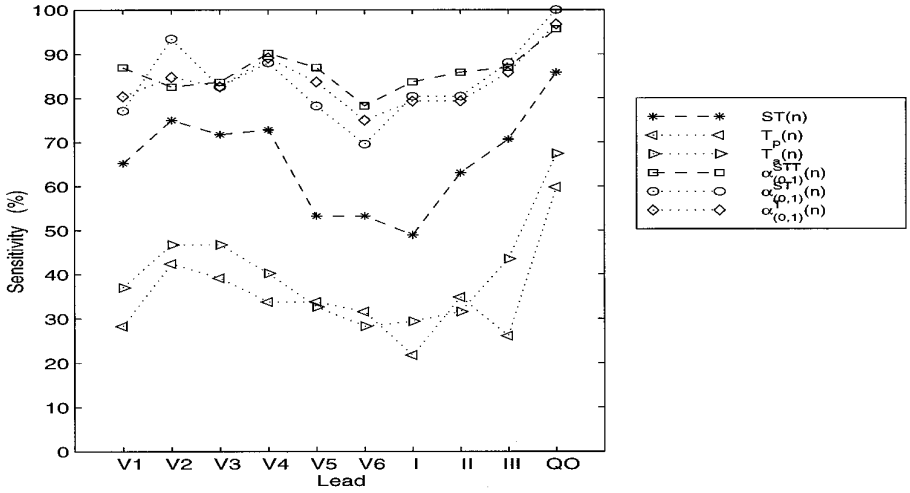

FIG. 11. Sensitivity to the ischemic-induced changes (averaged in all patients) for the different indexes and combinations of them, when $\eta = 4$ is selected.

change detection (see Fig. 11). The sensitivity improvement obtained by $\alpha_{0,1}^{\mathrm{STT}}$ index (85% of mean among leads and 96% for QO leads combination) with respect to local indexes (ST (64% mean, 86% for QO), T_{p} (33% mean, 60% for QO), and T_{a} (37% mean, 67% for QO) can be seen in Fig. 11 in which the dashed lines represent the best performance of local and global indexes ($\alpha_{0,1}^{\mathrm{STT}}$ and ST, respectively). This important result reveals that ventricular repolarization changes can be better detected using indexes that take into account global information from the entire ST–T complex than using local measurements. In fact, the KL-derived index corresponding to the entire ST–T complex (α^{STT}) had a higher sensitivity than those corresponding to the ST segment or T wave (α^{ST} or α^{T}, respectively), showing that the entire ST–T complex had been affected during the occlusion.

We have assumed that all the patients had changes in their ECGs as a response to the occlusion, but in several of them these effects could have been minimized by the presence of collateral flows, etc. Without this information it is not possible to consider the specificity problem. However, we can study the variation in the sensitivity with respect to the trade-off given not by the specificity (as would be desirable) but by the threshold value. We have applied different threshold values in the rule detection to calculate the dependence of the sensitivity on the threshold (see Fig. 12 for dependence in QO leads combination). Obviously, when η is increased the sensitivity level decreases.

Comparative Incidence of Ischemia at ST Level and T Wave

To study the incidence of ischemia on the different ECG intervals we used both the local and the KL-derived indexes following the decision rule described before to classify the different changes found during PTCA. We distinguished

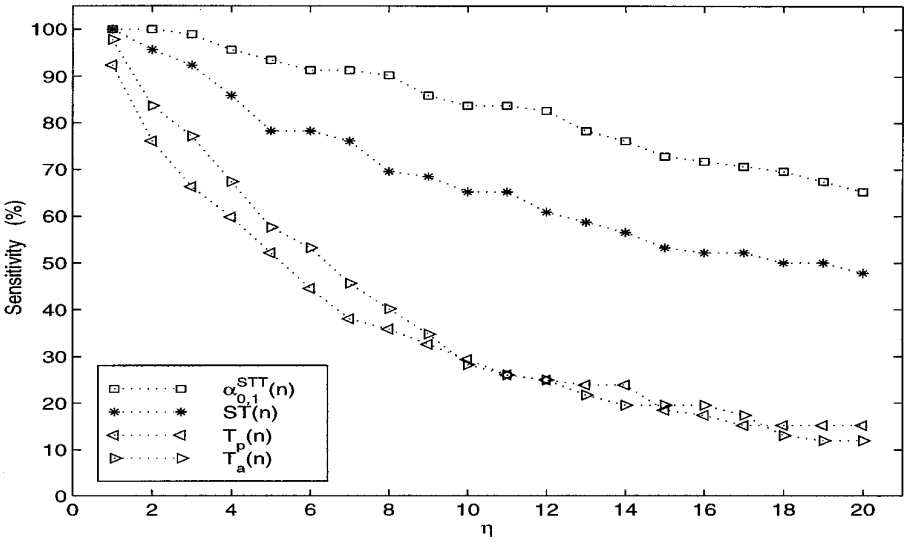

FIG. 12. Dependence of the sensitivity to induced ischemic changes on the η threshold.

among patients for which neither ST-level nor T-wave changes were detected (case 0,0), patients with T-wave but without ST-level changes (case 0,1), patients with ST-level but without T-wave changes (case 1,0), and cases with both ST-level and T-wave variations (case 1,1). In the first criterion, we used ST and $T_{(p,a)}$ (logical OR combination of T_p, T_a indexes) to decide if changes in ST segment and T wave, respectively, were found during PTCA. The results are shown in Fig. 13 (using $\eta = 4$). In most cases ST-segment changes were present accompanied by T-wave changes (37% of cases). In 26% of cases only ST deviations were found (case 1,0) and in 13% only T-wave changes (case 0,1). The results also reveal that leads V2, V3, and V4 showed the most sensitive response to induced ischemia (lower percentage of cases 0,0, 15%). In the second criterion, the decision rule was applied to the ICS parameters of $\alpha_{0,1}^{ST}$ and $\alpha_{0,1}^{T}$ indexes. The results are shown in Fig. 14. There were several differences in the classification given by the local measurements. There were fewer cases without any change than with the use of traditional indexes (8% vs 23% of case 0,0), as a result of the change detection increase when the global measurements were used. The (case 1,1) corresponding to changes detected throughout the ST–T complex was much larger (72%), and the (case 0,1) and (case 1,0) had the same occurrence (10%), showing that T-wave changes can be present (after the 4 min that the balloon typically was down) in the same percentage as ST deviations, indicative of the induced ischemia.

Case Study

Now we present a case that illustrates the fact that it is possible to find changes in the T-wave morphology without a significant ST level deviation. It also permits one to see that global indexes can provide useful information about those changes

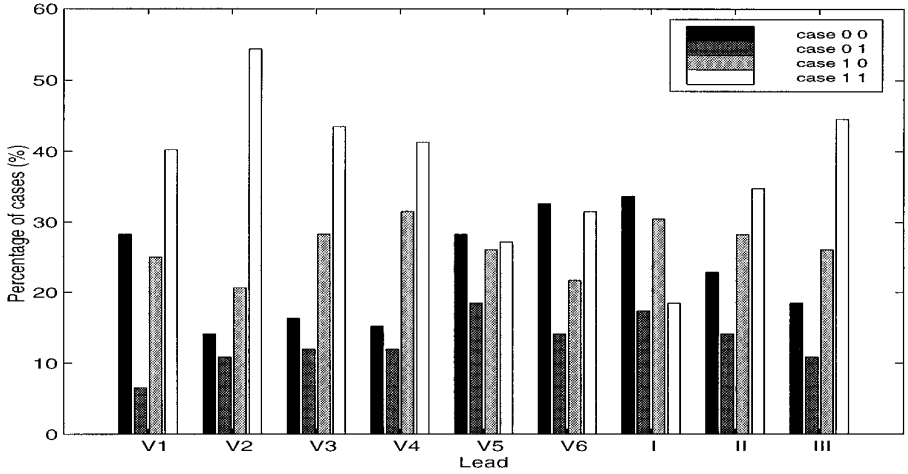

FIG. 13. Percentage of patients with different ST-segment/T-wave change patterns using the first criterion: ($T_{(p,a)}$ index) for T-wave and ST index for ST-level change detection.

in the whole ST–T complex. In Fig. 15 the trends for lead V5 of a patient who underwent an angioplasty are represented. The inflation period corresponds to the interval between the dash-dotted lines (occlusion time of 4 min 33 s). In this case the patient did not present significant ST elevation/depression:

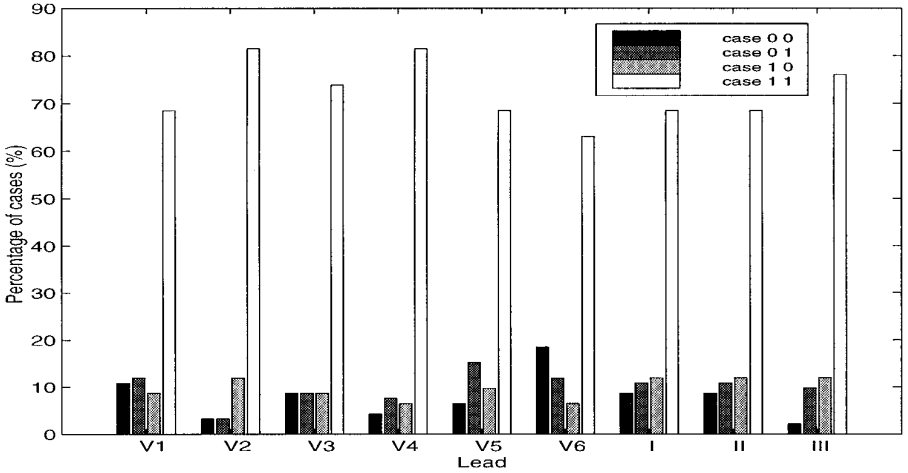

FIG. 14. Percentage of patients with different ST-segment/T-wave change patterns using the second criterion: $\alpha_{0,1}^{T}$ index for T-wave and $\alpha_{0,1}^{ST}$ index for ST-level change detection.

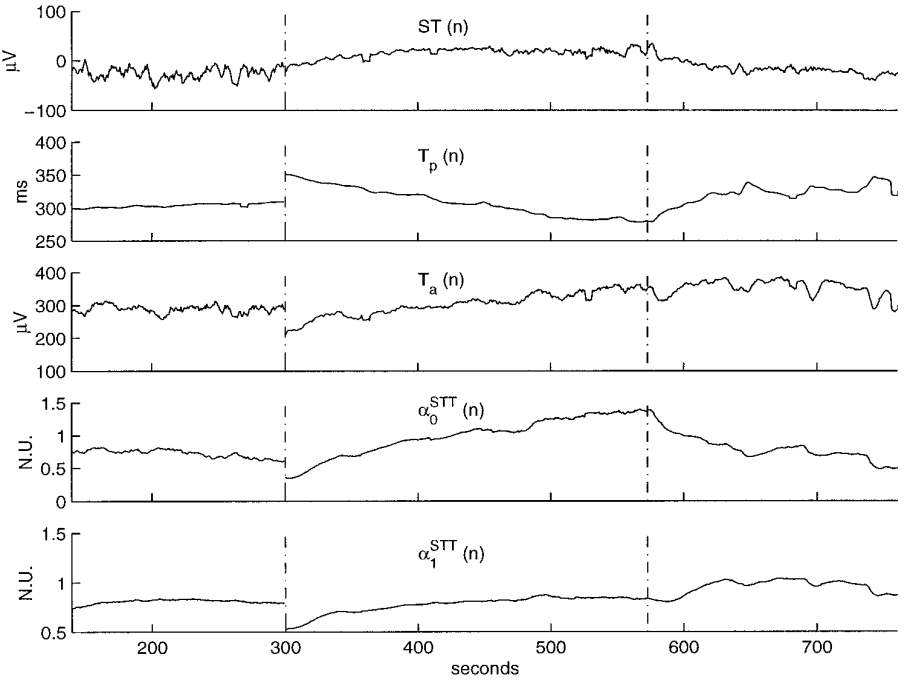

FIG. 15. Detail of series during PTCA (dash-dotted lines define the occlusion period.)

the estimated elevation was $\Delta ST = 22\ \mu V$. However it is evident from Fig. 15 that the ventricular repolarization has shown significant changes while the balloon was up in the other series. T-wave maximum position and amplitude series reflect these changes too: an increase of 115 μV in T-wave amplitude and a decrease of 73 ms in the maximum position were estimated, showing that there were significant changes in the T wave but not in the ST segment. It should be noted that the discontinuity in the series at the onset of PTCA appears because the angioplasty starts in a new ECG record, and probably displacements in the electrodes and the presence of the catheter, even with the balloon down, affected the ECG waveforms. The estimated variations during the angioplasty (Δindex) and the ICS parameter for traditional and global indexes are shown in Table 1, reflecting whether repolarization changes were detected. The ICS_{ST} parameter was unable to detect ischemic changes in this lead using $\eta = 4$. The use of global measurements as $\alpha_{(0,1)}^{STT}$ index allowed the detection of these changes that appear throughout the entire ST–T complex. This case has permitted us to illustrate the advantage of the use of global measurements that can account for changes present along the repolarization period and to show that changes in T wave can appear without ST-level deviations as a response to the ischemic conditions.

TABLE 1

Estimated Changes during PTCA (Δindex) and ICS Parameter for Each Index

	ST	T_p	T_a	α_0^{STT}	α_1^{STT}
Δindex	22 μV	−73 ms	115 μV	0.96 n.u.	0.26 n.u.
ICS_{index}	1.8	−12.7	4.1	9.4	3.5
Detection ($\eta = 4$)	No	Yes	Yes	Yes	No

DISCUSSION

We analyzed local and global measurements to determine which appeared to be the most sensitive in ischemic-induced change detection. All indexes were compared under similar performance conditions, selecting ΔSNR in the adaptively estimated KL coefficients that yielded convergence time equal to the number of beats averaged in the traditional measurements. Regarding the noise in the estimation of the time series, several measures were taken to reduce its effects. In local indexes signal averaging was applied and in global series the uncorrelated noise was removed using an adaptive filter. Moreover, the effect of high-frequency noise has small projection on the first $\alpha_i(n)$ series.

In the computer simulations it has been shown that two KL coefficient series permit us to track the signal evolution. In other applications such as ECG data compression the use of more basis functions could be needed to get a desired minimum reconstruction error (*18*).

In the study of global indexes we derived basis functions and the corresponding time series for ST segment, T wave, and ST–T complex. The α_i^{STT} indexes showed the best sensitivity to the induced changes. The KL-derived indexes for ST segment and T wave also showed high levels of sensitivity but their use is more restricted because of the difficulty in defining their locations (in fact, the ST and T windows were taken with a gap between them to avoid accounting for changes in one window due to the other). The series were estimated with and without Bazett's correction but no significant differences in the final sensitivity performance were found. This heart rate correction was used to normalize the windows because it is a much more stable measurement than T maximum or end of T can be. In long QT syndrome patients the representation could be not as adequate and perhaps basis functions of higher order would be needed, but even in this case tracking of signal changes may be possible. The low projection of the first basis functions over the final part of the ST–T complex could make it difficult to study changes in this last part with only the first two basis functions, and it may be necessary to use functions of higher order to detect them.

The results of detection percentage were also calculated using a different signal processing for the T-wave series ($T_p(n)$, $T_a(n)$). Instead of using the averaging, we tested a median filter of five samples in length that increased the detection percentage to values, in mean, from 33 to 49% for $T_p(n)$ and from 37 to 47% for $T_a(n)$. This significant increase is due to the better rejection of sudden transient

changes of T-wave morphology in the control recording obtained with the nonlinear filter, which resulted in a decrease of σ_{index} (and thus in an increase of the ICS parameter).

An important aspect is that changes detected by the $\alpha_i(n)$ time series reflect any kind of morphological changes, including local changes (level, position, or amplitude changes) and global changes (energy, morphology variations, etc.), getting more information from the ECG signal than isolated measurements. In this work it seems reasonable to assume that changes found in the repolarization are related to the occlusion and that all of these changes are ischemic induced. In a generic study (not under PTCA controlled conditions) the specificity problem should be added. In PTCA recordings we know inflation and deflation times that defined the intervals in which the ischemia was expected to appear and the efforts were only dedicated to study the indexes' response to the occlusion. In the general use of the method the detection of the timings in which the changes are present should be considered.

Finally, regarding the incidence of changes on the ST level and T wave, the main result was that ST level deviations and T-wave changes used to appear together, as a result of the ischemic-induced changes. It was also shown that T-wave changes could appear in an earlier phase of the ischemia (as the ''ischemic cascade'' hypothesis predicts), but a similar number of cases (using global indexes) with ST deviations and without T-wave changes was also found.

CONCLUSIONS

The results showed that $\alpha_{(0,1)}^{\text{STT}}$ index obtained the best sensitivity in detection of ischemic-induced changes (more than 85% of patients detected) compared to local measurements (64% using ST, 33% with T_{p}, and 37% with T_{a}). This reveals that ventricular repolarization changes can be better detected using indexes that get global information of the complex than using local measurements.

Both traditional and KL-derived indexes were used to classify the different changes found during PTCA. The results showed that in most of the cases (37% with local indexes and 72% with global indexes), when ST segment changes are present they are accompanied by T-wave changes, showing that repolarization changes are global variations of the entire period and not restricted only to ST segment. There were also found patients with changes in only one of the intervals: ST-segment deviations (26% with traditional indexes and 10% with global indexes) or T-wave changes (13% with traditional indexes and 10% with global indexes). The percentage of patients with no pattern of change using the KL-based indexes was lower (8%) than that obtained with the traditional measurements (23%), showing that the ischemic-induced changes were present throughout the ST–T complex and not only at specific locations.

APPENDIX: LIST OF SYMBOLS

$\mathbf{C}$	Covariance matrix
$\mathscr{E}$	Expected value

$\mathbf{x}$	Signal vector
$\mathbf{x}^{\mathrm{T}}$	Transpose signal vector
k	Sample index
α'	Nonnormalized KL coefficient vector
α_i	Normalized KL coefficient vector
i	KL basis function order
n	Occurrence time order (beat number)
n_0	Template beat
N	Signal length (number of samples)
E_n	Signal vector energy
τ_{mse}	MSE convergence time
ΔSNR	Signal-to-noise ratio improvement
$E_n^{\mathrm{P}}(i)$	Percentage of energy represented by the ith coefficient
$E_n^{\mathrm{C}}(i)$	Percentage of cumulative represented energy
$\phi_i^{\mathrm{T}}(k)$	KL basis functions for the T wave
$\phi_i^{\mathrm{ST}}(k)$	KL basis functions for the ST segment
$\phi_i^{\mathrm{STT}}(k)$	KL basis functions for the ST–T complex
$\alpha_i^{\mathrm{T}}(n)$	ith order KL time series for the T wave
$\alpha_i^{\mathrm{ST}}(n)$	ith order KL time series for the ST segment
$\alpha_i^{\mathrm{STT}}(n)$	ith order KL time series for the ST–T complex
$\mathrm{ST}(n)$	ST-level time series
$T_{\mathrm{p}}(n)$	T-wave maximum position time series
$T_{\mathrm{a}}(n)$	T-wave maximum amplitude time series
$\mathrm{ICS}_{\mathrm{index}}$	Ischemic changes sensor parameter of the index
Δindex	Estimated magnitude of change
σ_{index}	Standard deviation of the index
η	Threshold

ACKNOWLEDGMENTS

This work was supported in part by project TIC97-0945-C02-02 from CICYT (Spain). This study is part of the STAFF Studies.

REFERENCES

1. Birnbaum, Y., Sclarovsky, S., Blum, A., Mager, A., and Cabbay, U. Prognostic significance of the initial electrocardiographic pattern in a first acute anterior wall myocardial infarction. *Chest* **103,** 1681 (1993).
2. Kornreich, F., Macleod, R. S., Dzavik, V., *et al*. QRST changes during and after percutaneous transluminal coronary angioplasty. *J. Electrocardiol.* **27,** 113 (1994).
3. Wagner, N. B., Sevilla, D. C., Krucoff, M. W., Lee, K. L., Pieper, K. S., Kent, K. K., Bottner, R. K., Selvester, R. H., and Wagner, G. S. Transient alterations of the QRS complex and ST segment during percutaneous transluminal balloon angioplasty of the left anterior descending coronary artery. *Am. J. Cardiol.* **62,** 1038 (1988).
4. Abboud, S., Cohen, R. J., Selwyn, A., Ganz, P., Sadeh, D., and Friedman, P. L. Detection of transient myocardial ischemia by computer analysis of standard and signal-averaged high-frequency electrocardiograms in patients undergoing percutaneous transluminal coronary angioplasty. *Circulation* **76,** 585 (1987).

5. Pettersson, J., Warren, S., Mehta, N., Lander, P., Berbari, E., Gates, K., Sörnmo, L., Pahlm, O., Selvester, R. H., and Wagner, G. S. Changes in high-frequency QRS components during prolonged coronary artery occlusion in humans. *J. Electrocardiol.* **28,** 225 (1995).
6. Gallino, A., Chierchia, S., Smith, S., Croom, M., *et al*. Computer system for analysis of ST segment changes on 24 hour Holter monitor tapes: Comparison with other available systems. *J. Am. Coll. Cardiol.* **4,** 245 (1984).
7. Akselrod, S., and Norymberg, M., *et al*. Computerized analysis of ST segment changes in ambulatory electrocardiograms. *Med. Biol. Eng. Comput.* **25,** 513 (1987).
8. Puddu, P. E., and Bourassa, M. G. Prediction of sudden death from QTc interval prolongation in patients with chronic ischemic disease. *J. Electrocardiol.* **19,** 203 (1986).
9. Ahnve, S., Gilpin, E., Madsen, E. B., Froelicherand, V., Henning, H., and Ross, J. Prognostic importance of QT_c interval at discharge after acute myocardial infarction: A multicenter study of 865 patients. *Am. Heart J.* **108**(2), 395 (1984).
10. Laguna, P., Caminal, P., Thakor, N. V., and Jané, R. Automatic QT interval analysis in postmyocardial infarction patients. *J. Ambulatory Monitoring* **4,** 91 (1991).
11. Rosenbaum, D. S., Lange, M. D., *et al*. Electrical alternans and vulnerability to ventricular arrhythmias. *N. Engl. J. Med.* **330,** 235 (1994).
12. Smith, J. M., Blue, B., Clancy, E., Valeri, C. R., and Cohen, R. J. Subtle alternating electrocardiographic morphology as an indicator of decreased cardiac electrical stability. *In* ''Computers in Cardiology,'' pp. 109–112. IEEE Comput. Soc., Los Alamitos, CA, 1984.
13. Scher, A., Young, A., and Meredith, W. Factor analysis of the electrocardiogram. *Circ. Res.* **8,** 519 (1960).
14. Horan, L., Flowers, N., and Brody, D. Principal factor waveforms of the thoracic QRS complex. *Circ. Res.* **15,** 131 (1964).
15. Nygards, M. E., and Sörnmo, L. Delineation of the QRS complex using the envelope of the ECG. *Med. Biol. Eng. Comput.* **21,** 538 (1983).
16. Lux, R. L., Evans, A. K., Burgess, M. J., Wyatt, R. F., and Abildskov, J. A. Redundancy reduction for improved display and analysis of body surface potential maps. I. Spatial compression. *Circ. Res.* **49,** 186 (1981).
17. Evans, A. K., Lux, R. L., Burgess, M. J., Wyatt, R. F., and Abildskov, J. A. Redundancy reduction for improved display and analysis of body surface potential maps. II. Temporal compression *Circ. Res.* **49,** 197 (1981).
18. Olmos, S., Millán, M., García, J., and Laguna, P. ECG data compression with the Karhunen–Loève transform. *In* ''Computers in Cardiology 1996,'' pp. 253–256. IEEE Comput. Soc., Los Alamitos, CA, 1996.
19. Jager, F. J., Mark, R. G., Moody, G. B., and Divjak, S. Analysis of transient ST segment changes during ambulatory monitoring using the Karhunen–Loève transform. *In* ''Computers in Cardiology,'' pp. 691–694. IEEE Comput. Soc., Los Alamitos, CA, 1992.
20. Laguna, P., Moody, G. B., Jané, R., Caminal, P., and Mark, R. G. Karhunen–Loève transform as a tool to analyze the ST-segment. *J. Electrocardiol.* **28,** 41 (1996).
21. Therrien, C. W. ''Discrete Random Signals and Statistical Signal Processing.'' Prentice Hall, New York, 1992.
22. Laguna, P., Jané, R., Olmos, S., Thakor, N. V., Rix, H., and Caminal, P. Adaptive estimation of QRS complex by the Hermite model for classification and ectopic beat detection. *Med. Biol. Eng. Comput.* **34,** 58 (1996).
23. Moody, G. B., and Mark, R. G. Development and evaluation of a 2-lead ECG analysis program. *In* ''Computers in Cardiology,'' pp. 39–44. IEEE Comput. Soc., Los Alamitos, CA, 1982.
24. Laguna, P., Mark, R. G., Goldberger, A., and Moody, G. B. A database for evaluation of algorithms for measurement of QT and other waveform intervals in the ECG. *In* ''Computers in Cardiology,'' pp. 673–676. IEEE Comput. Soc., Los Alamitos, CA, 1997.
25. Meyer, C. R., and Keiser, H. N. Electrocardiogram baseline noise estimation and removal using cubic splines and state–space computation techniques. *Comput. Biomed. Res.* **10,** 459 (1977).
26. Bazett, H. C. An analysis of the time relation of electrocardiograms. *Heart* **7,** 353 (1920).

27. Pahlm, O., and Sörnmo, L. Data processing of exercise ECGs. *IEEE Trans. Biomed. Eng.* **BME-34,** 158 (1987).
28. Laguna, P., Jané, R., and Caminal, P. Automatic detection of wave boundaries in multilead ECG signals: Validation with the CSE database. *Comput. Biomed. Res.* **27,** 45 (1994).
29. Jané, R., Blasi, A., García, J., and Laguna, P. Evaluation of an automatic detector of waveforms limits in holter ECG with the QT database. *In* "Computers in Cardiology." IEEE Comput. Soc., Los Alamitos, CA, 1997.